

Computational and experimental insights into the chemosensory navigation of *Aedes aegypti* mosquito larvae

Eleanor K. Lutz^a, Tjinder S. Grewal^b, Jeffrey A. Riffell^a

^a*Department of Biology, University of Washington, Box 351800, Seattle, WA 98195, USA*
^b*Department of Biochemistry, University of Washington, Box 357350, Seattle, WA 98195, USA*

Abstract

Mosquitoes are prolific disease vectors that affect public health around the world. Although many studies have investigated search strategies used by host-seeking adult mosquitoes, little is known about larval search behavior. Larval behavior affects adult body size and fecundity, and thus the capacity of individual mosquitoes to find hosts and transmit disease. Understanding vector survival at all life stages is crucial for improving disease control. In this study we use experimental and computational methods to investigate the chemical ecology and search behavior of *Aedes aegypti* mosquito larvae. We first show that larvae do not respond to several olfactory cues used by adult *Ae. aegypti* to assess larval habitat quality, but perceive microbial RNA as a potent foraging attractant. Second, we demonstrate that *Ae. aegypti* larvae use chemokinesis, an unusual search strategy, to navigate chemical gradients. Finally, we use computational modeling to demonstrate that larvae respond to starvation pressure by optimizing exploration behavior —possibly critical for exploiting limited larval habitat types. Our results identify key characteristics of foraging behavior in an important disease vector mosquito. In addition to implications for better understanding and control of disease vectors, this work establishes mosquito larvae as a tractable model for chemosensory behavior and navigation.

Keywords: Mosquito, Behavior, *Aedes aegypti*, Larvae, Chemotaxis, Chemosensation

1 Introduction

The mosquito *Aedes aegypti* is a global vector of diseases such as Dengue, Zika, and Chikungunya [1]. This synanthropic mosquito is evolutionarily adapted to human dwellings, with some populations breeding exclusively indoors [2, 3]. The urban microhabitat features unique climatic regimes, photoperiod, and resource availability. In response to these selective pressures, successful synanthropic animals including cockroaches [4], rats [5], and crows [6] exhibit many behaviors absent in non-urbanized sibling species. Understanding these behaviors is of major importance to public health. Throughout human history, synanthropic disease vectors have caused devastating pandemics like the Black Death, which killed an estimated 30-40% of the Western European population [7, 8]. Like rats or cockroaches, adult *Ae. aegypti* mosquitoes exhibit many behavioral adaptations to human microhabitats [2, 9]. However, comparatively little is known about larval adaptations. The larval environment directly affects adult body size [10, 11], fecundity [11], and biting persistence [12], and understanding vector survival at all life stages is crucial for improving disease control [13]. Despite growing interest [14, 15, 16], it remains an open question how environmental stimuli affect larval behavior to regulate these responses and processes.

In addition to the above public health implications,

the behavior of synanthropic mosquito larvae is fascinating from a theoretical search strategy perspective. *Ae. aegypti* larvae are aquatic detritivores that live in constrained environments such as vases and tin cans [10]. In such limited environments, do larva exhibit a chemotactic search strategy (in which animals change their direction of motion in response to a chemical stimuli), or do they use a chemokinetic response (in which animals change a non-directional component of motion, such as speed or turn frequency, in response to a chemical stimuli) [17]? Mechanistic understanding of larval foraging behavior may provide insight into chemosensory systems controlling the behavior as well as the evolutionary adaptations for these systems in synanthropic environments.

In this work, we investigate larval *Ae. aegypti* behavior from a chemical ecological and search theory perspective. First, we explore the chemosensory cues involved in larval foraging. Although many olfactory cues are used by adult females to select oviposition sites [18], it is unclear if larvae and adults use the same chemicals to assess larval habitat quality. Second, we consider larval search behavior in spatially restricted environments using empirical data and computational modeling. Our work identifies the lack of chemotaxis in foraging *Ae. aegypti* larvae—an example of how environmental restrictions may drive the evolution of animal behavior. We further identify mi-

crobial RNA as a potent and unusual larval foraging attractant. Together, our results identify *Ae. aegypti* larvae as a tractable model in biological search theory, and highlights the importance of investigating synanthropic disease vectors at all life history stages.

Results

Effects of Sex, Physiological State, and Circadian Timing on Larval Physiology

Behavioral experiments in insects have demonstrated the importance of circadian timing, starvation, and age [19]. However, little is known about the effects of these variables on *Ae. aegypti* larvae. To better understand the effects of nutritional state and sex on our study organism, we used machine vision to track individual 4th instar *Ae. aegypti* larvae in a custom arena before each experiment (Fig 1A). For both fed and starved animals, female larvae were larger than males (fed larvae: n=135♀, 153♂, p<0.0001, effect size=0.53mm; starved larvae: n=89♀, 122♂, p<0.01, effect size=0.26mm, Fig S1A). Starved larvae were also smaller than fed animals for both females (p<0.0001, effect size=0.51mm) and males (p<0.01, effect size=0.23mm, Fig S1A). Because adult *Ae. aegypti* exhibit crepuscular activity [10], we also investigated the effects of circadian timing on larval behavior. We found no effects of circadian timing on larval movement speed (p=0.40), time spent moving (p=0.41), or time spent next to arena walls (p=0.55). These observations support previous findings that mosquito larvae, unlike adults, exhibit little behavioral variation during the day [20, 21].

Quantifying the Chemosensory Environment in Naturalistic Larval Habitat Sizes

Previous research has shown that other species of mosquito larvae detect many different chemosensory stimuli [23]. In *Ae. aegypti*, it is unclear what chemical signals cues, if any, larvae use to navigate their environment. Nevertheless, chemosensory cues may be essential in avoiding predation or foraging efficiently. Using our arena and machine vision methods, we investigated larval preference for eight six putatively attractive and aversive chemosensory cues sets of stimuli. First, we experimentally verified the chemical diffusion in the arena and found that larval movement significantly increased the diffusion of stimuli within the arena (p<0.0001, Fig S2). We next created a chemical diffusion map for analyzing stimuli preference using only experiments containing larvae (Fig 1B, Fig S2A-D). For chemosensory stimuli, we used predicted attractive stimuli including a 0.5% mixture of food (Hikari Tropic First Bites fish food) suspended in water, as well as food extract filtered through a 0.2μm filter to remove solid particulates. Quinine was used as a putative aversive stimulus (a bitter tastant aversive to many insects including *Drosophila melanogaster*

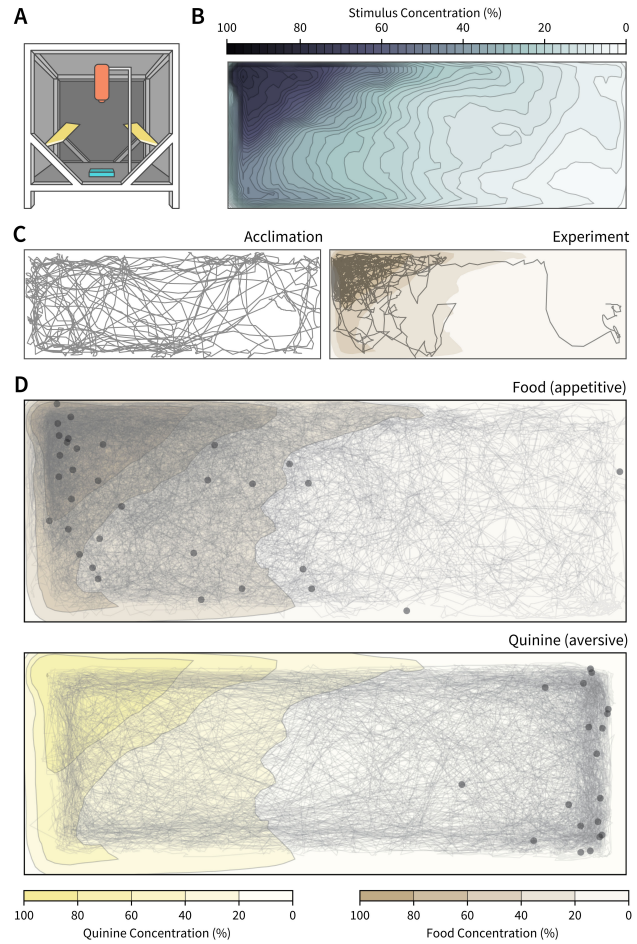


Figure 1: Quantifying the chemosensory environment in naturalistic larval habitat sizes. **A:** Diagram of experimental conditions, adapted from [22], including a Basler Scout Machine Vision GigE camera (orange), infrared lighting (yellow) and a behavior arena (blue). **B:** Chemosensory diffusion map of the behavior arena at the end of the 15 minute experiment. **C:** Example of an individual larval trajectory during the 15 minute acclimation phase (left). Trajectory of same individual during the 15 minute experiment phase, responding to food added to the left side of the arena (right). **D:** Trajectory of all starved animals presented with food (top) or quinine (bottom). Although trajectories are shown aggregated into one image, all animals were tested individually. Scatter points show the position of each animal at the end of the experiment and color overlays show the chemosensory diffusion map at the end of the 15 minute experiment.

and *Apis mellifera* [24, 25]). We also tested indole and o-cresol, two microbial compounds that attract adult mosquitoes for oviposition [26]. Finally, we tested the response of larvae to RNA, glucose, and a mixture of 9 amino acids required for *Ae. aegypti* larval growth. All three components are essential for *Ae. aegypti* survival [27], and RNA polynucleotides serve as attractants or essential nutrients for larvae of other mosquito species [28, 29, 30, 31]. Moreover, dissolved RNA is released at high levels ($\mu\text{g L}^{-1} \text{ h}^{-1}$) from growing populations of microbes in freshwater habitats [32], and could provide valuable foraging information to omnivores such

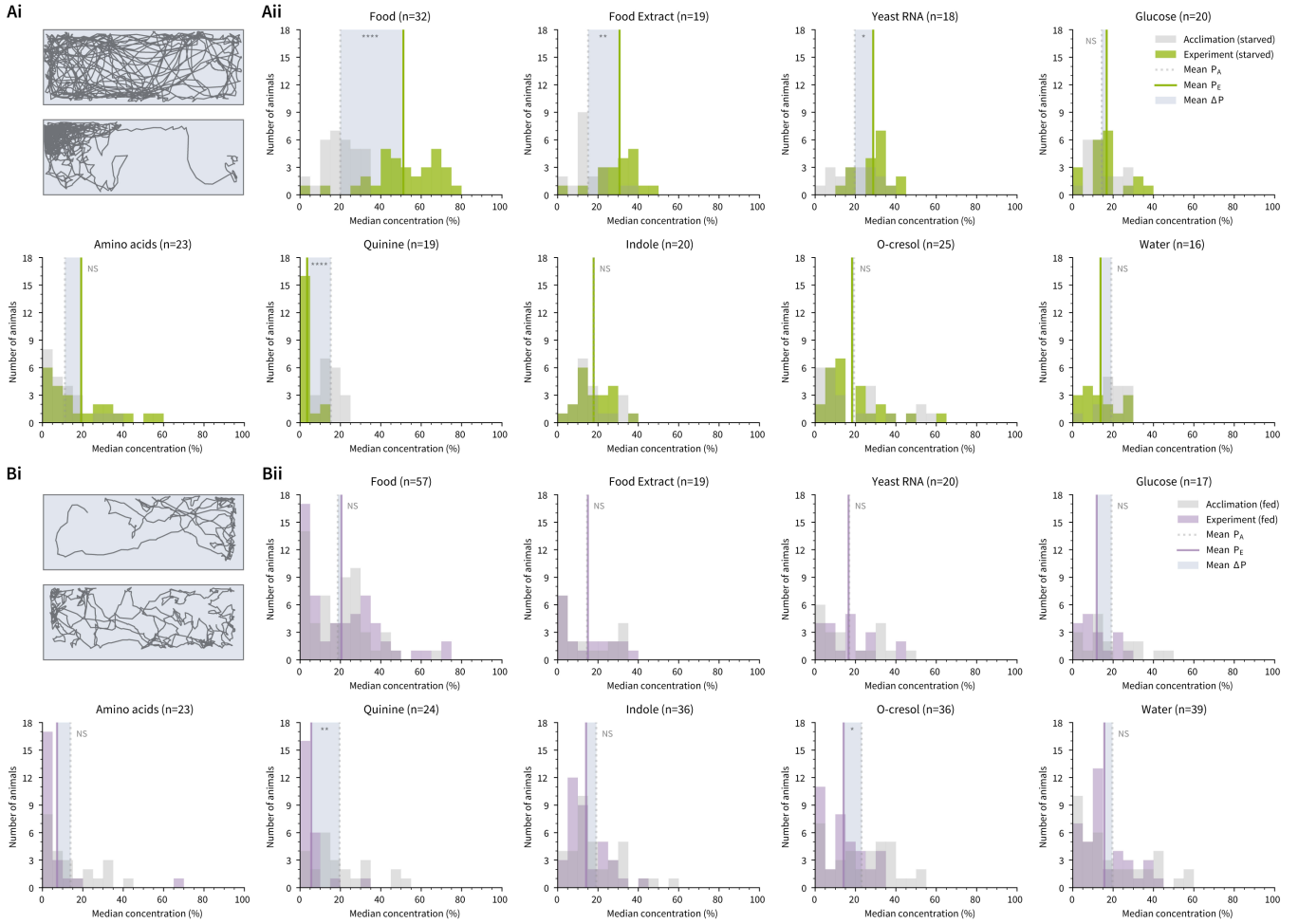


Figure 2: Physiological feeding state affects larval attraction towards ecologically relevant odors. **Ai:** Example trajectory of a starved larva during the acclimation (top) and the experiment phase (below), responding to food introduced to the top left. **Aii:** Distribution of larvae during the acclimation phase (grey) and experiment phase (green), median concentration. The shaded box visualizes the mean ΔP across all individuals. Note that due to the unequal distribution of high and low concentration areas in the behavior arena, animals naturally appear to distribute near lower concentrations when no stimulus is present. **Bi:** Example trajectory of a fed larva during the acclimation (top) and experiment phase (below), responding to food introduced to the top left. **Bii:** Distribution of fed larval preference during the acclimation (grey) and experiment phase (purple). In Aii and Bii, asterisks denote the significance level of paired-sample Welch's t-tests comparing acclimation P and experiment P (NS: not significant). N values reported next to each stimulus describe the number of animals in the treatment.

	Potential Chemosensory Search Strategies				Experiment Observations
	Anosmic	Chemotaxis	Klinokinesis	Chemokinesis	
Stimulus preference ΔP	no	yes	yes	yes	yes ($p < 0.0001$)
Directional preference ΔDP	no	yes	no	no	no ($p = 0.98$)
Δ Concentration speed ΔDS	no	no	no	no	no ($p = 1$)
Concentration speed ΔCS	no	no	no	yes	yes ($p < 0.0001$)
Δ Concentration turns ΔDTI	no	yes	no	no	no ($p = 1$)
Concentration turns ΔCTI	no	no	yes	no	no ($p = 1$)

Table 1: Comparing larval exploration behavior to canonical animal search strategy models. Four different chemosensory search strategies are listed (central columns) along with the expected observable behavior metrics for each strategy (left column). By comparing the experimental observations (right column) with the expected results, we determined that *Ae. aegypti* larval chemosensory navigation is best explained by an chemokinesis search strategy model.

as *Ae. aegypti*. By contrast, other isolated macronutrients such as salts, sugars, and amino acids elicit little to no attraction in other larval mosquito species [33].

125 Physiological Feeding State Affects Larval Attraction
126 Towards Ecologically Relevant Odors
127 For each of these seven eight sets of stimuli, in ad-
128 dition to water, we compared the stimulus preference

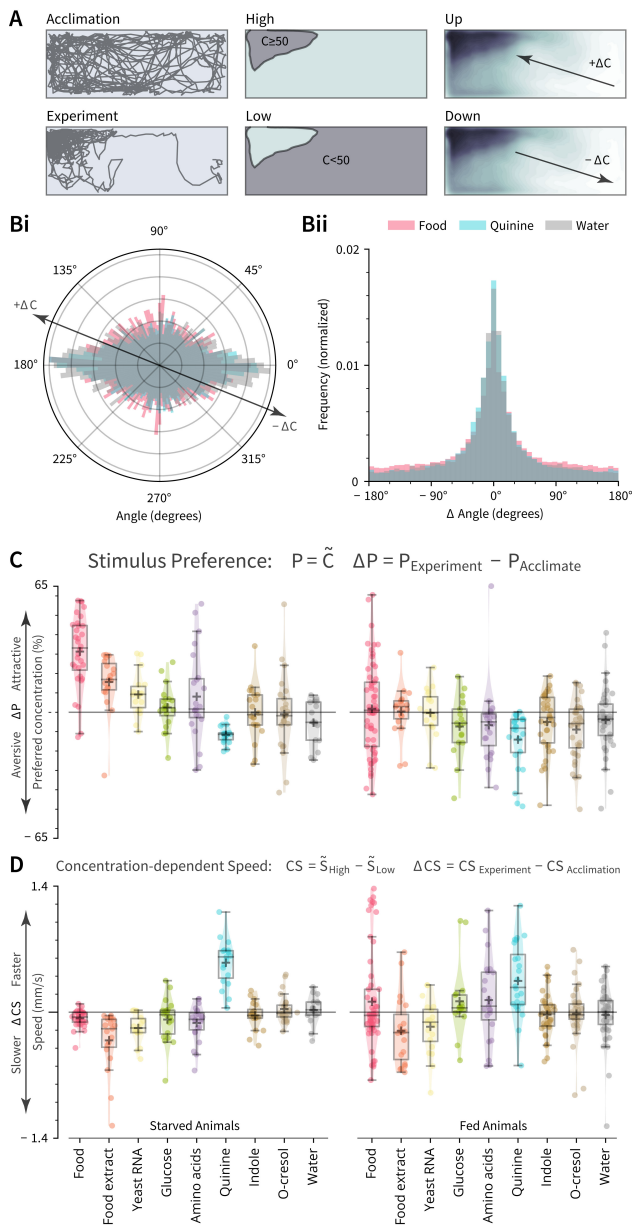


Figure 3: Larval exploration behavior is best explained by a chemokinesis search model. **A:** Diagram of behavioral quantifications. Larvae were observed during a 15-minute acclimation period in clean water, followed by a 15-minute experiment in the presence of the stimulus. The arena was divided into an area of high ($\geq 50\%$) and low concentration ($< 50\%$). Larvae could move in a direction that increased local concentration ($+ \Delta C$) or decreased local concentration ($- \Delta C$). **Bi:** Orientation of animals in the arena throughout the experiment. Larvae did not exhibit directional movement in response to appetitive or aversive stimuli. Note that larvae spend more time moving horizontally ($0^\circ, 180^\circ$) because the rectangular arena is longer in the horizontal direction. **Bii:** Larvae did not change frequency of turns (ΔAngle) in response to appetitive or aversive stimuli. **C:** Box plots for the population median ± 1 quartile, population mean (+ marker) and mean response for each individual (dots) for larval preference (ΔP). A horizontal line at 0 represents no change in behavior following stimulus addition. **D:** As in C, except for stimulus-dependent changes in Concentration-dependent Speed (ΔCS).

of larvae before and after stimulus addition (Fig 1C, Fig 2A, Fig S3, Fig S4, Fig S5). Preference was defined as the median concentration chosen by the larvae throughout the 15-minute experiment, normalized to behavior during the previous 15-minute acclimation phase. Starved larvae were attracted to food ($n=32$, $p<0.0001$) and spent significantly less time near the aversive cue quinine ($n=19$, $p<0.0001$). Food extract filtered through a $0.2\mu\text{m}$ filter remained attractive ($n=19$, $p=0.004$), suggesting that larvae use small, waterborne chemical cues to forage. To further investigate these foraging cues, we next examined responses to microbial RNA, glucose, and an amino acid mixture. We found that RNA was significantly attractive ($n=18$, $p=0.049$), while glucose ($n=20$, $p=1$), and the amino acid mixture ($n=23$, $p=1$) were not. Addition of water —a negative control for mechanical disturbance—had no impact on larval positional preference ($n=16$, $p=1$). Although we expected indole and o-cresol, which are attractive to adult *Ae. aegypti*, to elicit attraction from larvae, neither odorant elicited a change in behavior from the acclimation phase (indole: $n=20$, $p=1$; o-cresol: $n=25$, $p=1$). Indole tested at a higher concentration (10mM) also had no effect ($n=19$, $p=0.31$). Together, these results suggest that larvae and adults may not necessarily rely on similar cues to assess larval habitat quality.

The physiological feeding state of an adult mosquito has a strong impact on subsequent behavioral preferences [34], but it remains unknown how feeding status influences responses to chemosensory stimuli in larvae. We thus fed larvae ad libitum to fish food before testing their responses to each of the seven chemosensory cues eight stimuli and a water control (Fig 2B). Fed larvae showed no significant attraction to food ($n=57$, $p=1$), food extract ($n=19$, $p=1$), and RNA ($n=20$, $p=1$), supporting the prediction that microbial RNA functions as an attractant in the context of foraging. Nonetheless, fed larvae still exhibited aversive responses to quinine ($n=24$, $p=0.003$), demonstrating that the lack of response to foraging cues is not due to a global reduction in chemosensory behavior. Similar to starved larvae, fed animals showed no preference for the water control ($n=39$, $p=1$), indole (100 μM : $n=36$, $p=0.98$; 10mM: $n=17$, $p=1$), glucose ($n=17$, $p=1$), or the amino acid mixture ($n=23$, $p=1$). Fed larvae exhibited significant aversion to o-cresol ($n=36$, $p=0.026$).

A Chemokinesis Navigation Strategy is Most Consistent with Larval Aggregation Toward Cues Investigated in this Study

Next we investigated the behavioral mechanism by which *Ae. aegypti* larvae locate sources of odor, since such information could provide insight into the chemosensory pathways that mediate the behaviors.

We hypothesized that larval aggregation near attractive cues such as food is mediated by chemotaxis—a common form of directed motion observed in many animals and microbes [35, 36, 37]. In chemo-klinotaxis (hereafter chemotaxis), animals exhibit directed motion with respect to a chemical gradient. Alternatively, larvae may exhibit chemo-ortho-kinesis (hereafter chemokinesis) —a process in which animals respond to local conditions by regulating speed rather than direction—or chemo-klino-kinesis (hereafter klinokinesis) —in which animals respond to local conditions by regulating turning frequency. Finally, larvae may be unable to detect chemosensory stimuli, and thus exhibit purely random behavior (hereafter anomeric). To differentiate between these strategies, we quantified six observable metrics used to characterize navigation behavior (Table 1). By breaking down larval trajectories into several different components (Fig 3A-B) and identifying which variables correlate with stimulus preference (Fig 3C-D), we can infer which search strategy best explains larval behavior.

Surprisingly, we found no evidence for chemotaxis near attractive or aversive chemicals. Starved larvae did not exhibit kinematic changes characteristic of chemotaxis, such as directional preference (ΔDP , $p=0.98$, Fig 3Bi, Fig S6A). Further, larvae could not increase odor localization efficiency above random chance: discovery time for all cues was comparable across treatments (ΔD , $p=1$, Fig S6B). Larvae also did not perform klinokinesis: Turning frequency was unaffected by either the instantaneous concentration the larvae experienced (ΔCTI , $p=1$, Fig 3Bii, Fig S6C) or change in concentration (ΔDTI , $p=1$, Fig S6D). Instead, we found that larval activity was most consistent with chemokinesis **for the eight cues tested in these experiments**. Larvae altered movement speed when experiencing high local stimuli conditions (ΔCS , $p<0.0001$, Fig 3D) but not when moving up or down the concentration map (ΔDS , $p=1$, Fig S6E). When grouped into aversive, attractive, and neutral chemosensory cues, the correlation between preference (ΔP) and chemokinetic response (ΔCS) similarly separated into three clusters (Fig S7). We did not observe a strong linear relationship in our dataset, perhaps because the majority of cues tested did not elicit a strong behavioral preference.

230 Starved *Ae. aegypti* Optimize Exploration Behavior to 231 Increase the Probability of Finding Food

232 Many organisms change their speed or activity rate
233 when starved [38], and we predicted that starved
234 *Ae. aegypti* may also alter their exploration behavior
235 to increase the probability of discovering food. Experimental
236 observations showed evidence for starvation-mediated
237 behavior changes—starved animals spent more time exploring ($p<0.0001$, Fig 4A) and spent less time near walls and corners ($p<0.0001$, Fig 4B).

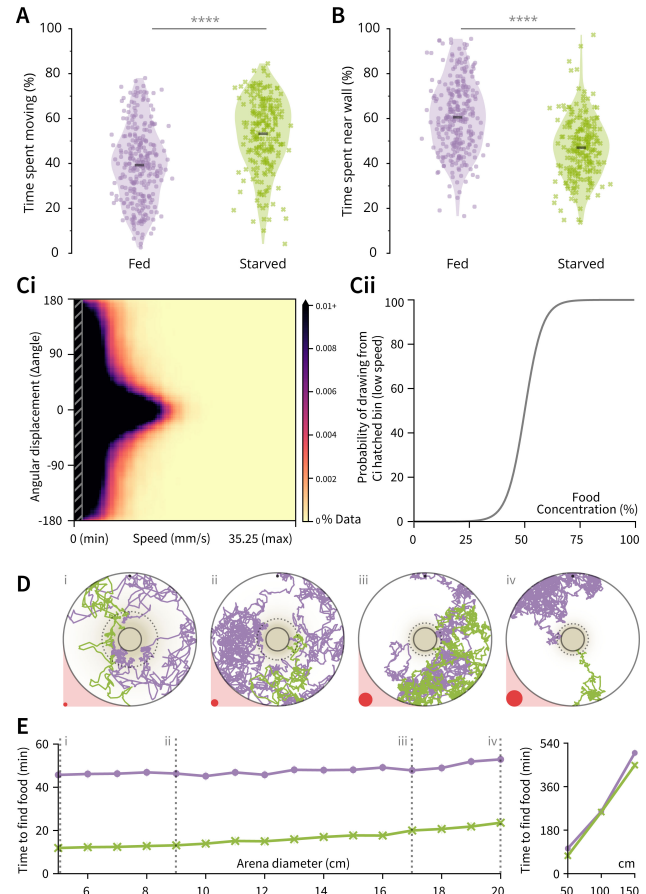


Figure 4: Starved *Ae. aegypti* optimize exploration behavior to increase the probability of finding food. **A:** Starved larvae spend more time exploring the arena than fed larvae. **B:** Starved larvae spend less time within one body length of an arena wall. **(A,B)** Violin plot. Dots are the means for each individual, and black bar is the mean across all individuals ($n>168$ per treatment); asterisks denote $p<0.0001$ (Welch's t-test). **C:** We developed a computational model to approximate the chemokinetic behavior observed in experimental data. **Ci:** Probability Density Function of the relationship between movement speed and instantaneous angle for starved animals. The shaded grey rectangle to the left visualizes the area encompassing half of the available data. **Cii:** Trajectories were constructed by sampling values from the shaded rectangle when larvae were in areas of high food concentration, and sampling values from outside the shaded rectangle when in areas of low food concentration. The probability function for drawing from the two distributions was smoothed to avoid threshold artifacts. **D:** Simulated trajectories of fed (purple) and starved (green) larvae foraging in ecologically relevant arena sizes. Relative size of each arena is visualized as red circles. In this figure larvae began at the top center (fed) or the bottom center (starved). However in actual simulations starting location was randomized for each individual. **Di:** 5cm, **Dii:** 9cm, **Diii:** 17cm, and **Div:** 20cm simulated arena diameters. In all cases, the solid black circle outlines the food target goal, and the dashed circle represents the boundary of 50% food concentration. **E:** Simulated chemokinetic larvae using empirical data from starved animals (green, X markers) found the food source consistently faster than the same model using data from fed animals (purple, dots). Mean of 1000 simulations \pm standard error. Dashed grey lines correspond to ecologically relevant habitat sizes described in Table S1 and in D.

We were interested in understanding whether or not these behavioral changes might be adaptive in ecologically relevant container sizes. We thus created two chemokinesis foraging models using empirical data from fed and starved animals ($n=248$ fed larvae during the acclimation phase; $n=445,925$ trajectory data points; $n=168$ starved larvae during the acclimation phase; $n=302,096$ trajectory data points). This computational model explored circular arenas of various ecologically relevant diameter sizes **5 to 20cm in diameter** (Table S1) by randomly sampling instantaneous speed and turn angle from experimental data (Fig 4C). Individual simulations using this model were tasked with finding a food source at the center of one of these arenas (Fig 4D), starting from a randomized location. Similar to the trajectories of starved larvae (Fig 2D), our simulated trajectories exhibited tortuous paths that ultimately encountered the food patch. Nonetheless, the chemokinesis model using empirical data from starved animals discovered the food source more than 20 minutes faster than fed animals across all habitat sizes (Fig 4E), supporting our hypothesis that starvation-mediated changes in larval behavior increase the probability of finding food in larval environments. Moreover, **all** simulated starved larvae could find the food source in under 25 minutes across **these smaller all environment sizes** (Fig 4E). Given that *Ae. aegypti* larvae can survive up to a week without food [10], our results suggest that a chemokinetic search strategy is sufficient to successfully forage in diverse and realistic larval habitats. **Although our simulation assumptions are less suitable for understanding larger breeding sites¹, we further simulated habitats 50, 100, and 150cm in diameter for comparison.** We found that larvae still discovered the food source in several hours (fed simulations: 1.7, 4.3, and 8.3 hours; starved simulations: 1.2, 4.2, and 7.5 hours for 50, 100, and 150cm arenas, Fig 4E). Finally, the slope for starved animals **in smaller habitats** was about twice that of fed animals (starved: $45.3 \text{ seconds} \cdot \text{cm}^{-1}$; fed: $22.9 \text{ s} \cdot \text{cm}^{-1}$), suggesting that the benefit of behavioral modification in starved animals is more pronounced in smaller arena sizes (slope of difference between fed - starved simulations: $-22.4 \text{ s} \cdot \text{cm}^{-1}$).

Discussion

In this study we quantify essential characteristics of *Ae. aegypti* larval behavior that are crucial for the development of future studies. Further, we identify previously unknown behaviors that highlight the unique evolutionary history and developmental biology of these disease vector mosquitoes. First, we show

that larvae perceive microbial RNA as a foraging attractant, but do not respond to several olfactory cues that attract adult *Ae. aegypti* for oviposition. Second, we demonstrate that *Ae. aegypti* larvae use chemokinesis, rather than chemotaxis, to navigate with respect to chemical sources. Finally, we use experimental observations and computational analyses to demonstrate that larvae respond to starvation pressure by changing their behavior to increase the probability of finding food sources in realistic habitat sizes.

Although adult *Ae. aegypti* feeding is regulated by ATP perception [39], we are unaware of other work demonstrating **perception of nucleotides or nucleic acids such as RNA RNA attraction** in *Ae. aegypti* larvae. In our state-dependent preference experiments, we investigate the ecological basis of larval RNA attraction, and propose that RNA may function as **one of the a foraging indicators** in the larval environment. However, **44 different nutrients are required for *Ae. aegypti* larval survival** [27], and the attractiveness of other potential phagostimulants including vitamins and carbohydrates have not been tested with the sensitivity of our experimental methods. In addition, the concentration and relative composition of phagostimulants may have complex effects on larval preference, and these combinatorial effects were not examined in this study. In a natural environment *Ae. aegypti* larvae likely rely on a combination of stimuli to locate food sources. **Although the receptor responsible for RNA detection is unknown, work in *D. melanogaster* suggests that a gustatory or ionotropic receptor may be more likely candidates than an olfactory receptor.** In addition Nevertheless, an earlier study demonstrated that olfactory receptor deficient (*orco* $-/-$) *Ae. aegypti* larvae showed no defects in attraction to food **or avoidance of quinine** [22]. Taken together, our results support the hypothesis that sensory information gained from gustatory or ionotropic receptors may be more integral to larval chemosensation than olfactory receptors. Further, larval attraction to RNA suggests that the importance of nucleotide phagostimulation is preserved throughout a mosquito's life cycle, from larval foraging to adult blood engorgement and oviposition.

Our study also raises a number of comparative questions that could be addressed in future research. For instance, is chemokinesis in mosquito larvae associated with human association and man-made containers? Future studies could compare chemotactic ability in other spatially constrained mosquitoes, such as *Toxorhynchites* (which inhabit tree holes) or *Aedes albopictus* (another container-breeding mosquito) [40], to species that oviposit in larger bodies of water such as *Aedes togoi* (marine rock pools) or opportunistic species such as *Culex nigripalpus* that oviposit in a wide range of habitat sizes [40, 41]. Additionally, computational modeling of fluid dynamics and larval move-

¹Large breeding sites are probably more likely to contain multiple small patches of food distributed throughout the environment, rather than our simulated model of one single patch.

ment may help determine whether chemotaxis is physiologically and physicochemically challenging in small, man-made environments. Due to the diffusive environment in the small containers, where shallow gradients dominate and turbulence is lacking, the change in time or space of the chemical signal may be too small for the larvae to detect. This is particularly relevant considering our results showing that larval movement significantly modifies the stimulus gradient [42].

Synanthropic mosquitoes are increasingly important to global health as urbanization progresses: Currently over half of all humans live in urban environments, and this proportion is only expected to increase [43]. Adaptations that facilitate human cohabitation, like specialized larval foraging strategies, are vital to our understanding of mosquito behavior and success as a disease vector [9].

Materials and Methods

Details on the Insects, Selection of Preparation of Odorants, and Statistical Analyses, can be found in the Electronic Supplementary Materials.

Behavior Arena and Experiment

We previously developed a paradigm to investigate chemosensory preference in larval *Ae. aegypti* [22]. In this study we expanded our protocol by mapping the chemosensory environment in our arena using fluorescein dye. Importantly, because larval swimming activity increases chemical movement within the arena, we mapped the dye distribution from experiments containing an actively swimming larva. 100 μ L of fluorescein dye was added to a white arena of the same material and dimensions, each containing one *Ae. aegypti* larva. Dye color was converted to concentration values using a standardization dataset of 13 reference concentrations (Fig S2C). Dye diffusion through time was quantified by the mean of all values in each 1mm² area, linearly interpolated throughout time (n=10, Fig S2B).

During behavior experiments, we recorded animals for 15 minutes before each experiment to analyze baseline activity and confirm that the arena was fair in the absence of chemosensory cues. Subsequently, 100 μ L of a chemical stimulus was gently pipetted into the left side of the arena to minimize mechanosensory disturbances, and larval activity was recorded for another 15 minutes (Fig 1C).

Video Analyses

Video data was obtained and processed as previously described [22] using Multitracker software by Floris van Breugel [44] and Python version 3.6.2. Additionally, approximate larval length was measured for each animal in ImageJ Fiji [45], as the pixel length from head to tail, in a selected video frame that showed the

larva in a horizontal position. Lengths were converted to mm using the known inner container width as the conversion ratio. Experimenters were blind to larval sex when measuring lengths. Throughout our analyses, the arena was divided into areas of high concentration ($\geq 50\%$ initial stimulus) and low concentration ($< 50\%$). Larvae could move in a direction that increased local concentration or decreased local concentration. We discounted concentration changes caused by diffusion while the larvae remained immobile. A threshold of $\Delta 2\%/\text{s}$ was required to qualify as moving up or down the concentration map.

Computational Modeling

We developed a chemokinetic computational model to investigate larval foraging success in different environments. This model resampled the observed trajectories of *Ae. aegypti* larvae to investigate the consequences of a chemokinetic search strategy using realistic larval behavioral metrics. In the experimental foraging task, simulated animals explored a circular arena until they encountered a food source at the center of the arena. These arenas included a range of 19 16 different arena sizes representing the range of many of the ecologically realistic habitats reported in literature (Table S1). The food target was scaled to arena size (comprising 3% of total area) under the assumption that habitats of larger diameter would also contain higher absolute amounts of food. Each simulated larvae began at a random point within the arena, and then explored the environment at each time step by sampling a paired speed-angle data point from experimental data (Fig 4Ci). We elected to pair these data points in our model because we observed that the two variables were correlated at higher speeds (Fig 4Ci). The time step was re-sampled if the selected data point would cause the trajectory of the simulated larvae to leave the boundary of the experimental arena. Data from animals tested with glucose and amino acids were not included. These experiments were conducted during the manuscript review process, and it was not possible to rerun simulations in the allotted time. Nevertheless, our simulations were sampled from over 700,000 data points from 416 individual larvae. To approximate chemokinetic behavior, simulated larvae in areas of high food concentration ($\sim > 50\%$) moved slower and turned more frequently. L, and larvae in areas of low food concentration ($\sim \leq 50\%$) moved faster and in a straighter line. These differences were implemented by splitting the paired speed-angle data into two bins of equal size, with one bin containing the slowest half of all data points and the other containing the faster half. The probability of sampling from each half was determined as a function of the instantaneous food concentration (Fig 4Cii), with the addition of an exponentially smoothed decision boundary to reduce thresholding artifacts. The empirical data pairs used

457 in these models represented all data taken from larvae
458 observed in clean water before the addition of experimental stimuli, with fed simulations sampling data
459 from fed animals and starved simulations sampling data from starved animals only (n=248 fed, n=168
460 starved). To define the boundary of 50% food concentration for chemokinetic behavioral decisions, we
461 defined the simulated chemical conditions using an exponential regression model of distance and concentration
462 based on our empirical chemical map (Fig S2E). When the simulated larvae entered the food patch at
463 the center of the arena, the simulation was stopped and the time taken to discover the food was recorded
464 (in seconds). We conducted 1,000 simulations for each arena size and nutritional state (fed vs. starved).

472 Acknowledgements

473 This work was supported in part by grants from the National
474 Institute of Health grant 1RO1DCO13693 and 1R21AI137947
475 to J.A.R.; National Science Foundation grants IOS-1354159 to
476 J.A.R. and DGE-1256082 to E.K.L.; Air Force Office of Sponsored
477 Research under grant FA9550-16-1-0167 to J.A.R.; and the Robin Mariko Harris Award to E.K.L. We thank Floris van
478 Breugel for assistance with video data analysis, the University
479 of Washington Biostatistics Consulting Group for statistical advice,
480 and Binh Nguyen and Kara Kiyokawa for maintaining the
481 Riffell lab mosquito colony. We also thank Thomas Daniel,
482 Bingni Brunton, Kameron Harris, and the Kincaid 320 Python
483 Club for insightful discussions on programming and data management.
484 Finally, we thank two anonymous reviewers for their
485 contribution of time, expertise, and thoughtful advice that significantly
486 improved this manuscript.

488 Author Contributions

489 Conceptualization: E.K.L. and J.A.R.; Methodology: E.K.L.
490 and J.A.R.; Software: E.K.L.; Investigation: E.K.L. and T.S.G.;
491 Resources: E.K.L. and J.A.R.; Data Curation: E.K.L; Writing
492 —Original Draft: E.K.L; Writing —Review and Editing: E.K.L,
493 J.A.R., and T.S.G.; Visualization: E.K.L; Supervision: J.A.R;
494 Project administration: J.A.R; Funding acquisition: E.K.L. and
495 J.A.R.

496 Declaration of Interests

497 The authors declare no competing interests.

498 Additional Files

499 Data and code associated with this manuscript can be found at
500 <https://github.com/eleanorlutz/aedes-aegypti-2019>

References

- [1] S. C. Weaver, C. Charlier, N. Vasilakis, M. Lecuit, Zika, Chikungunya, and other emerging vector-borne viral diseases, *Annu. Rev. Med.* 69 (2018) 395–408.
- [2] J. R. Powell, W. J. Tabachnick, History of domestication and spread of *Aedes aegypti*—a review, *Mem. Inst. Oswaldo Cruz.* 108 (2013) 11–17.
- [3] J. E. Brown, B. R. Evans, W. Zheng, V. Obas, L. Barrera-Martinez, A. Egizi, H. Zhao, A. Caccone, J. R. Powell, Human impacts have shaped historical and recent evolution in *Aedes aegypti*, the Dengue and yellow fever mosquito, *Evolution.* 68 (2) (2014) 514–525.
- [4] C. Schapheer, G. Sandoval, C. A. Villagra, Pest cockroaches may overcome environmental restriction due to anthropization, *J. Med. Entomol.* 55 (5) (2018) 1357–1364.
- [5] A. Y. T. Feng, C. G. Himsworth, The secret life of the city rat: A review of the ecology of urban Norway and black rats (*Rattus norvegicus* and *Rattus rattus*), *Urban Ecosyst.* 17 (1) (2014) 149–162.
- [6] J. M. Marzluff, K. J. McGowan, R. Donnelly, R. L. Knight, Causes and consequences of expanding American crow populations, in: J. M. Marzluff, R. Bowman, R. Donnelly (Eds.), *Avian Ecology and Conservation in an Urbanizing World*, Springer US, Boston, MA, 2001, pp. 331–363.
- [7] K. P. Aplin, H. Suzuki, A. A. Chinen, R. T. Chesser, J. Ten Have, S. C. Donnellan, J. Austin, A. Frost, J. P. Gonzalez, V. Herbreteau, F. Catzeflis, J. Soubrier, Y. Fang, J. Robins, E. Matisoo-Smith, A. D. S. Bastos, I. Maryanto, M. H. Sinaga, C. Denys, R. A. Van Den Bussche, C. Conroy, K. Rowe, A. Cooper, Multiple geographic origins of commensalism and complex dispersal history of black rats, *PLoS One.* 6 (11) (2011) e26357.
- [8] D. Raoult, G. Aboudharam, E. Crubézy, G. Larrouy, B. Ludes, M. Drancourt, Molecular identification by “suicide PCR” of *Yersinia pestis* as the agent of medieval black death, *Proc. Natl. Acad. Sci. U.S.A.* 97 (23) (2000) 12800–12803.
- [9] D. J. Gubler, E. E. Ooi, S. Vasudevan, J. Farrar, *Dengue and Dengue Hemorrhagic Fever*, 2nd Edition, CABI, 2014.
- [10] S. Christophers, *Aedes aegypti* (L.) the Yellow Fever Mosquito: Its Life History, Bionomics and Structure, Cambridge University Press, 1960.
- [11] H. Briegel, Metabolic relationship between female body size, reserves, and fecundity of *Aedes aegypti*, *J. Insect Physiol.* 36 (3) (1990) 165–172.
- [12] R. S. Nasci, Influence of larval and adult nutrition on biting persistence in *Aedes aegypti* (Diptera: Culicidae), *J. Med. Entomol.* 28 (4) (1991) 522–526.
- [13] E. K. Lutz, C. Lahondère, C. Vinauger, J. A. Riffell, Olfactory learning and chemical ecology of olfaction in disease vector mosquitoes: A life history perspective, *Curr. Opin. Insect Sci.* 20 (2017) 75–83.
- [14] J. J. Skiff, D. A. Yee, Behavioral differences among four co-occurring species of container mosquito larvae: Effects of depth and resource environments, *J. Med. Entomol.* 51 (2) (2014) 375–381.
- [15] M. H. Reiskind, M. Shawn Janairo, Tracking *Aedes aegypti* (Diptera: Culicidae) larval behavior across development: Effects of temperature and nutrients on individuals’ foraging behavior, *J. Med. Entomol.* 55 (5) (2018) 1086–1092.
- [16] J. B. Z. Zahouli, B. G. Koudou, P. Müller, D. Malone, Y. Tano, J. Utzinger, Urbanization is a main driver for the larval ecology of *Aedes* mosquitoes in arbovirus-endemic settings in south-eastern Côte d’Ivoire, *PLoS Negl. Trop. Dis.* 11 (7) (2017) e0005751.
- [17] S. Benhamou, P. Bovet, How animals use their environment: A new look at kinesis, *Anim. Behav.* 38 (3) (1989) 375–383.
- [18] S. G. Pavlovich, C. L. Rockett, Color, bacteria, and mosquito eggs as ovipositional attractants for *Aedes aegypti* and *Aedes albopictus* (Diptera: Culicidae), *Great Lakes Entomol.* 33 (2) (2018) 7.
- [19] M. Kaiser, M. Cobb, The behaviour of *Drosophila melanogaster* maggots is affected by social, physiological and temporal factors, *Anim. Behav.* 75 (5) (2008) 1619–1628.
- [20] R. Van Pletzen, Larval and pupal behavior in *Culiseta longiareolata*, *J. Limnol. Soc. S. Afr.* 7 (1) (1981) 24–28.
- [21] J. R. Clopton, A circadian rhythm in spontaneous locomotor activity in the larvae and pupae of the mosquito, *Culiseta incidens*, *Physiol. Entomol.* 4 (3) (1979) 201–207.
- [22] M. Bui, J. Shyong, E. K. Lutz, T. Yang, M. Li, K. Truong, R. Arvidson, A. Buchman, J. A. Riffell, O. S. Akbari, Live calcium imaging of *Aedes aegypti* neuronal tissues reveals differential importance of chemosensory systems for life-history-specific foraging strategies, *BMC Neurosci.* 20 (27) (2019).
- [23] Y. Xia, G. Wang, D. Buscariollo, R. J. Pitts, H. Wenger, L. J. Zwiebel, The molecular and cellular basis of olfactory-driven behavior in *Anopheles gambiae* larvae, *Proc. Natl. Acad. Sci. U.S.A.* 105 (17) (2008) 6433–6438.
- [24] C. Rusch, E. Roth, C. Vinauger, J. A. Riffell, Honeybees in a virtual reality environment learn unique combinations of colour and shape, *J. Exp. Biol.* 220 (19) (2017) 3478–3487.
- [25] A. El-Keredy, M. Schleyer, C. König, A. Ekim, B. Gerber, Behavioural analyses of quinine processing in choice, feeding and learning of larval *Drosophila*, *PLoS One.* 7 (7) (2012) e40525.
- [26] A. Afify, C. G. Galizia, Chemosensory cues for mosquito oviposition site selection, *J. Med. Entomol.* 52 (2) (2015) 120–130.
- [27] Singh, Brown, Nutritional requirements of *Aedes aegypti* l., *J. Ins. Physiol* 1 (1957) 199–220.
- [28] E. Barber, Herskowitz, The attraction of larvae of *Culex pipiens quinquefasciatus* say to ribonucleic acid and nucleotides, *J. Ins. Physiol* 28 (7) (1982) 585–588.
- [29] Dadd, Kleinjan, Phagostimulation of larval *Culex pipiens* l. by nucleic acid nucleotides, nucleosides and bases, *Physiol. Entomol* 10 (1) (1985) 37–44.
- [30] C. Ellgaard, Barber, Preferential accumulation of *Culex quinquefasciatus* (Diptera: Culicidae) larvae in response to adenine nucleotides and derivatives, *J. Med. Entomol* 24 (6) (1987) 633–636.

- [31] Dadd, Nucleotide, nucleoside and base nutritional requirements of the mosquito *Culex pipiens*, *J. Insect Physiol.* 25 (4) (1979) 353–359.
- [32] J. Paul, W. Jeffrey, J. Cannon, Production of dissolved DNA, RNA, and protein by microbial populations in a Florida reservoir, *Appl Environ Microbiol.* 56 (10) (1990) 2957–2962.
- [33] R. W. Merritt, R. H. Dadd, E. D. Walker, Feeding behavior, natural food, and nutritional relationships of larval mosquitoes, *Annu. Rev. Entomol.* 37 (1992) 349–376.
- [34] W. Takken, J. J. A. van Loon, W. Adam, Inhibition of host-seeking response and olfactory responsiveness in *Anopheles gambiae* following blood feeding, *J. Insect Physiol.* 47 (3) (2001) 303–310.
- [35] H. C. Berg, D. A. Brown, Chemotaxis in *Escherichia coli* analyzed by three-dimensional tracking, *Nature.* 239 (5374) (1972) 500–504.
- [36] G. Röder, M. Mota, T. C. J. Turlings, Host plant location by chemotaxis in an aquatic beetle, *Aquat. Sci.* 79 (2) (2017) 309–318.
- [37] Y. H. Hussain, J. S. Guasto, R. K. Zimmer, R. Stocker, J. A. Riffell, Sperm chemotaxis promotes individual fertilization success in sea urchins, *J. Exp. Biol.* 219 (10) (2016) 1458–1466.
- [38] M. de Jager, F. Bartumeus, A. Kölzsch, F. J. Weissing, G. M. Hengeveld, B. A. Nolet, P. M. J. Herman, J. van de Koppel, How superdiffusion gets arrested: Ecological encounters explain shift from Lévy to Brownian movement, *Proc. Biol. Sci.* 281 (1774).
- [39] R. Galun, L. C. Koontz, R. W. Gwadz, J. M. C. Ribeiro, Effect of ATP analogues on the gorging response of *Aedes aegypti*, *Physiol. Entomol.* 10 (3) (1985) 275–281.
- [40] D. F. Hoel, P. J. Obenauer, M. Clark, R. Smith, T. H. Hughes, R. T. Larson, J. W. Diclaros, S. A. Allan, Efficacy of ovitrap colors and patterns for attracting *Aedes albopictus* at suburban field sites in north-central Florida, *J. Am. Mosq. Control Assoc.* 27 (3) (2011) 245–251.
- [41] M. Bentley, Chemical ecology and behavioral aspects of mosquito oviposition, *Annu. Rev. Entomol.* 34 (1) (1989) 401–421.
- [42] A. M. Hein, D. R. Brumley, F. Carrara, R. Stocker, S. A. Levin, Physical limits on bacterial navigation in dynamic environments, *J. R. Soc. Interface.* 13 (114) (2016) 20150844.
- [43] M. A. Goddard, A. J. Dougill, T. G. Benton, Scaling up from gardens: Biodiversity conservation in urban environments, *Trends Ecol. Evol.* 25 (2) (2010) 90–98.
- [44] F. van Breugel, A. Huda, M. H. Dickinson, Distinct activity-gated pathways mediate attraction and aversion to CO₂ in *Drosophila*, *Nature.* 564 (7736) (2018) 420–424.
- [45] J. Schindelin, I. Arganda-Carreras, E. Frise, V. Kaynig, M. Longair, T. Pietzsch, S. Preibisch, C. Rueden, S. Saalfeld, B. Schmid, J.-Y. Tinevez, D. J. White, V. Hartenstein, K. Eliceiri, P. Tomancak, A. Cardona, Fiji: An open-source platform for biological-image analysis, *Nat. Methods.* 9 (7) (2012) 676–682.
- [46] K. L. Chan, B. C. Ho, Y. C. Chan, *Aedes aegypti* (L.) and *Aedes albopictus* (Skuse) in Singapore City. 2. Larval habitats, *Bull. World Health Organ.* 44 (5) (1971) 629–633.
- [47] C. Vinauger, E. K. Lutz, J. A. Riffell, Olfactory learning and memory in the disease vector mosquito *Aedes aegypti*, *J. Exp. Biol.* 217 (13) (2014) 2321–2330.
- [48] R core team (2013). R: A language and environment for statistical computing. <http://www.R-project.org/>. Accessed: 2019-3-18.

Supplementary Materials

Supplementary Data and Code

All code is available for download at github.com/eleanorlutz/aedes-aegypti-2019

Supplementary Figures

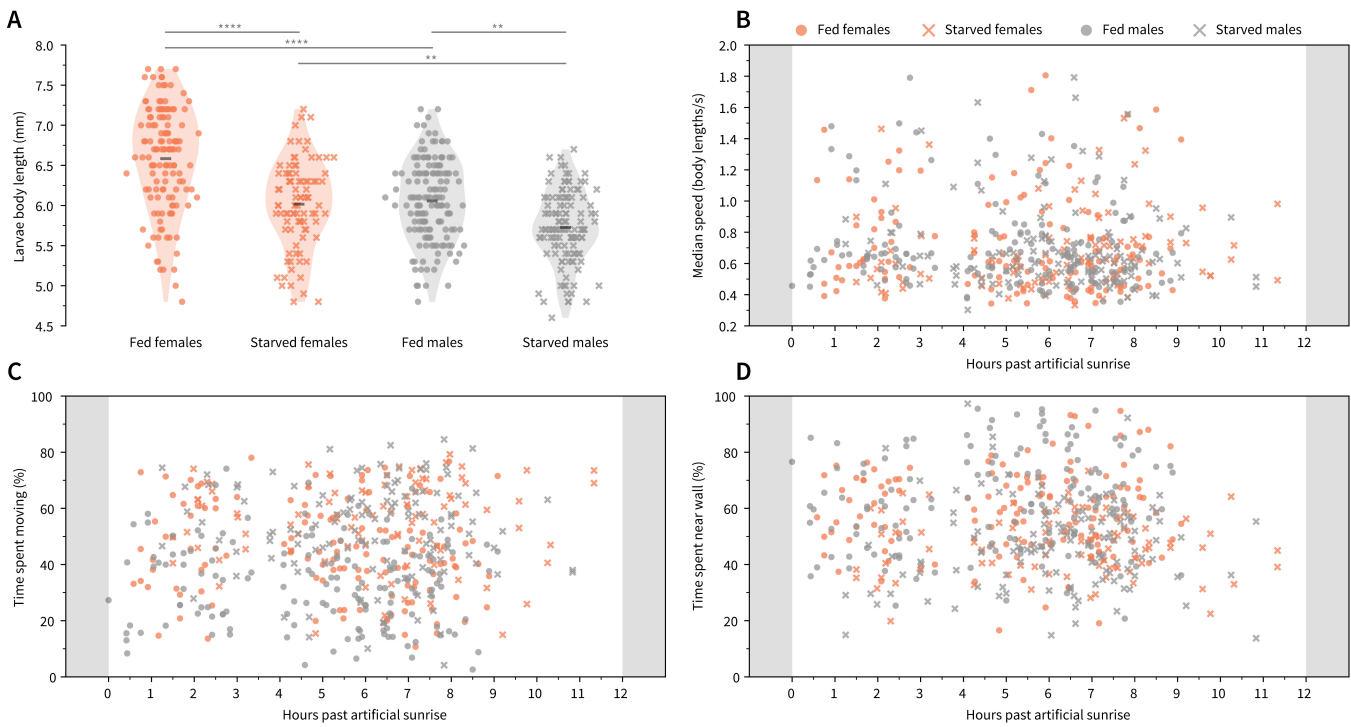


Figure S1: Effects of sex, physiological state, and circadian timing on larval physiology. **A-D:** Fed females (orange dots, $n=135$) and males (grey dots, $n=153$), starved females (orange X markers, $n=89$) and males (grey X markers, $n=122$). **A:** Violin plot. Scatter points show the body length (mm) for each individual, and the black bar is the mean across all individuals; asterisks denote significance values (Welch's t-test). Larval body length is influenced by sex and starvation state. **B:** No change was observed in median speed (body lengths/s) as a function of circadian timing. Note that the sampling rate throughout the day was not consistent due to the work schedule of experimenters involved in the project. **C:** No change was observed in time spent moving throughout daylight hours. **D:** No change was observed in proportion of time spent within one body length of the wall throughout daylight hours. **A-D:** For all effects shown above, we pooled measurements of all animals from the acclimation period. Our experiment results for each individual stimulus have far fewer animals for each sex, and we did not have sufficient power to analyze stimulus-specific sex differences. Nevertheless, we accounted for possible sex-specific confounds such as larval size or movement speed by normalizing the stimulus response of each animal to its activity during the pre-experiment acclimation period. In addition, we have included the sex information for each animal in our open-source code and data. We hope that the availability of this data can help inform researchers developing future experiments, even if statistical comparisons of stimulus response cannot be drawn with our current sample size.

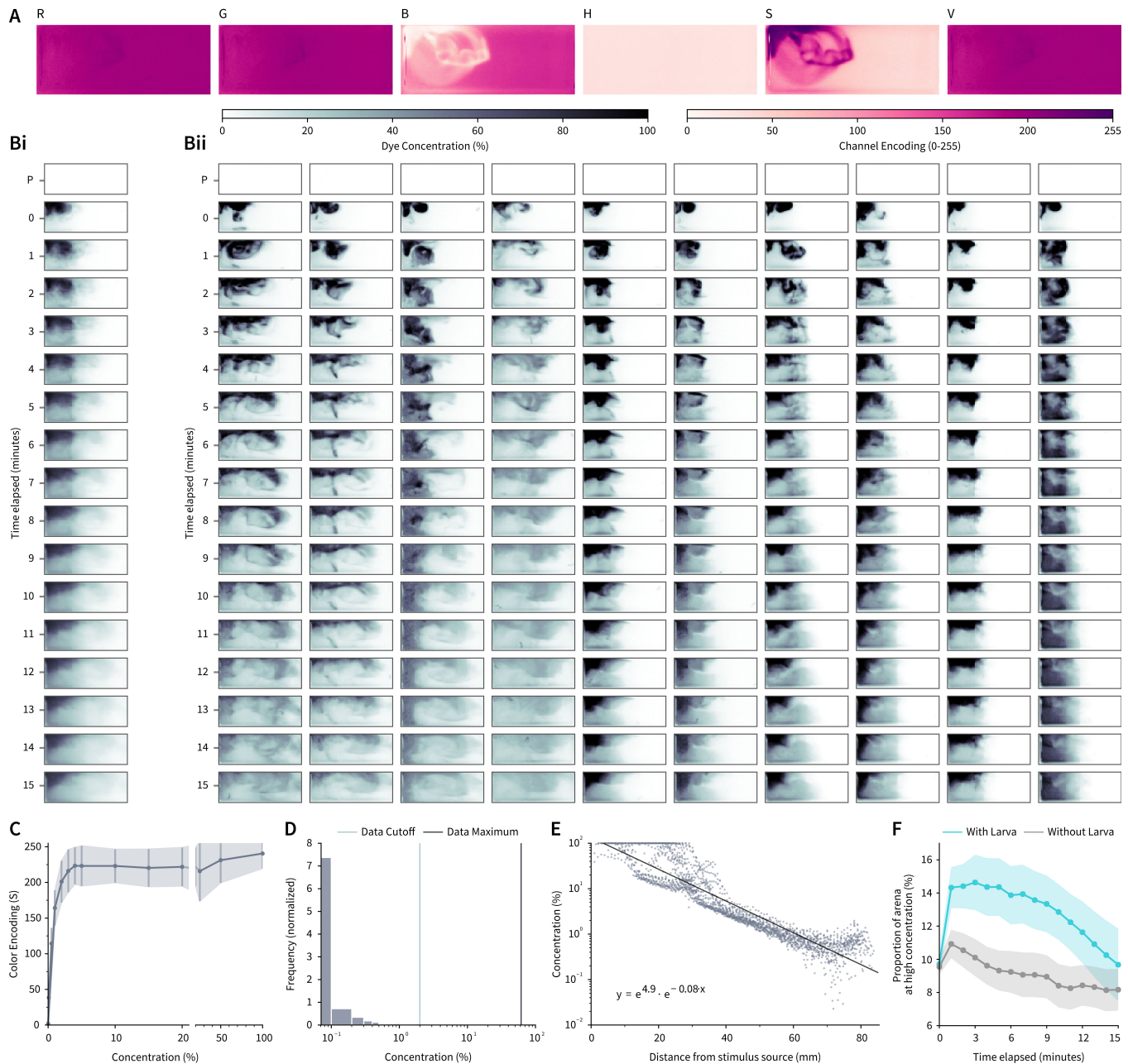


Figure S2: Creating a concentration gradient map to analyze and model larval search behavior. **A:** To quantify fluorescein dye diffusion, photographs were taken every minute using a Canon PowerShot ELPH 320 HS camera. Of the available color information channels (RGB, HSV), the saturation channel (S) contained the most information and was used to represent dye color throughout image analyses. **Bi:** Dye diffusion through time was quantified by the mean of all values in each 1mm^2 area, linearly interpolated through time ($n=10$ experiments containing larvae). A control photograph was taken before the start of each experiment (P) but was not used to construct the chemical gradient map. **Bii:** Individual variation between trials. Each column represents data from one experiment through time. **C:** Dye color (S) was converted to raw concentration values using a standardization dataset of 13 reference concentrations. 20mL of each reference concentration was poured into the entire arena and photographed. **D:** Because $100\mu\text{L}$ of dye is immediately diluted in the 20mL behavior arena water volume, reference concentration colors could not be used to directly convert color to % maximum concentration. Instead, the maximum concentration value was normalized to $\geq 95\%$ of all color measurements across all experiments. **E:** To create a concentration map for computational simulations in different arena sizes, we analyzed the relationship between concentration and distance from stimulus source at time=0. Concentration values for individual $1\times 1\text{mm}^2$ sections across all 10 experiments at time=0 (dots), best fit line (black). **F:** Presence of a larva within the container significantly increases the spread of fluorescein dye. As a proxy for dye distribution, we measured the proportion of 1mm^2 segments within the arena with a concentration of $>50\%$. Blue: Proportion of $>50\%$ segments in experiments with larvae; Gray: Proportion of $>50\%$ segments in experiments without larvae ($n=10$ each, mean \pm standard error). Initial dye distribution (time=0) was not significantly different between treatments, suggesting that subsequent observation differences are not due to experimenter bias in dye addition ($p=0.76$, Mann-Whitney U test). Linear regression of dye distribution for all subsequent time steps (time>0) showed significant differences between containers with and without larvae ($p<0.0001$).

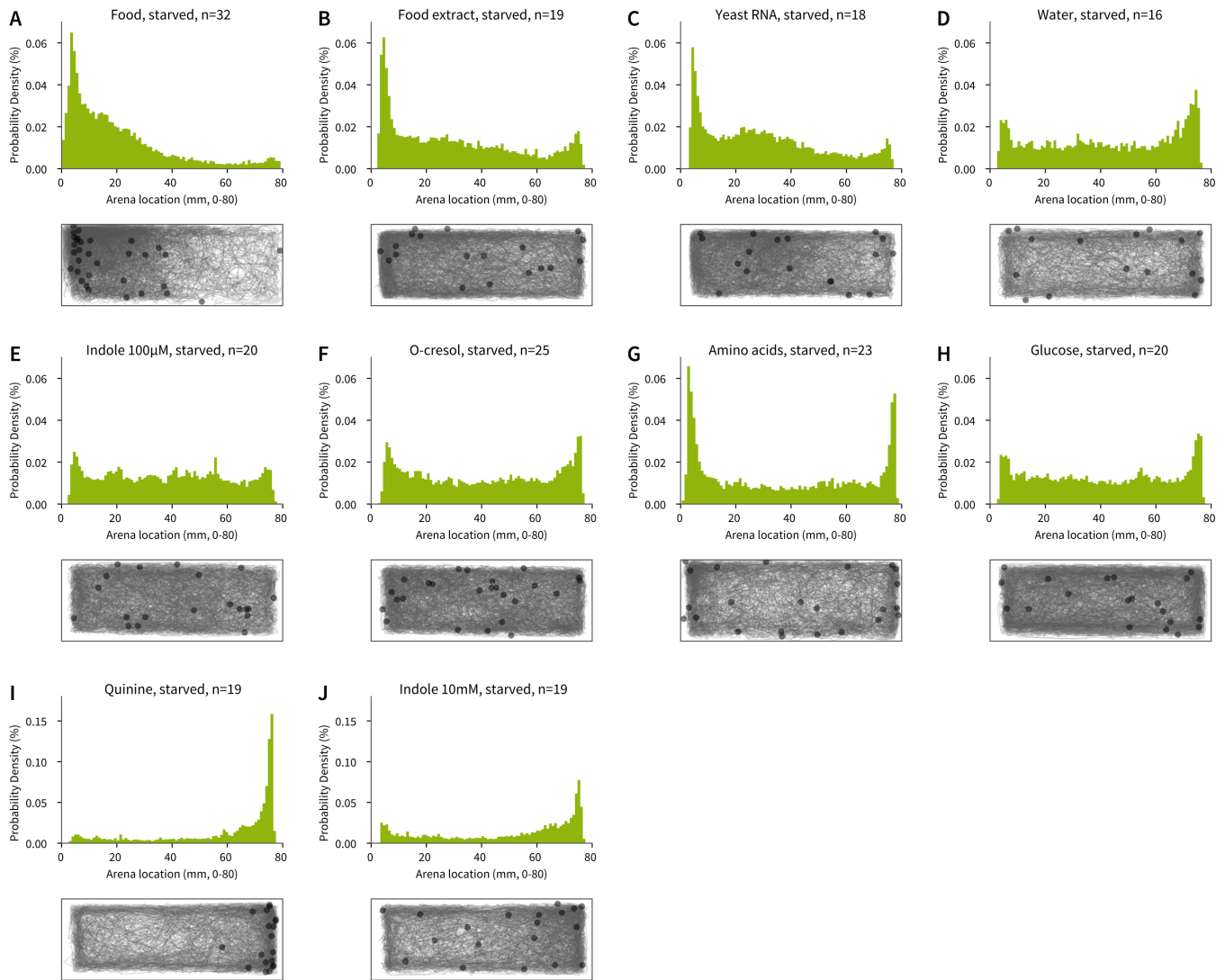


Figure S3: Response of starved larvae to experimental stimuli. A-J: Distribution and trajectories of all starved animals during the experiment phase for food (A), food extract (B), yeast RNA (C), water (D), 100 μ M indole (E), o-cresol (F), amino acid mixture (G), glucose (H), quinine (I), and 10mM indole (J). Although trajectories are shown aggregated into one image for each panel, all animals were tested individually. Scatter points show the position of each animal at the end of the experiment. It is important to note that these histograms show the aggregated position data from all animals throughout the entire 15-minute experiment. Thus, a single animal exhibiting strong attraction or aversion may disproportionately influence this data visualization. For statistical tests reported in this paper, a single preference value was calculated for each animal (Figure 3C) to avoid such effects.

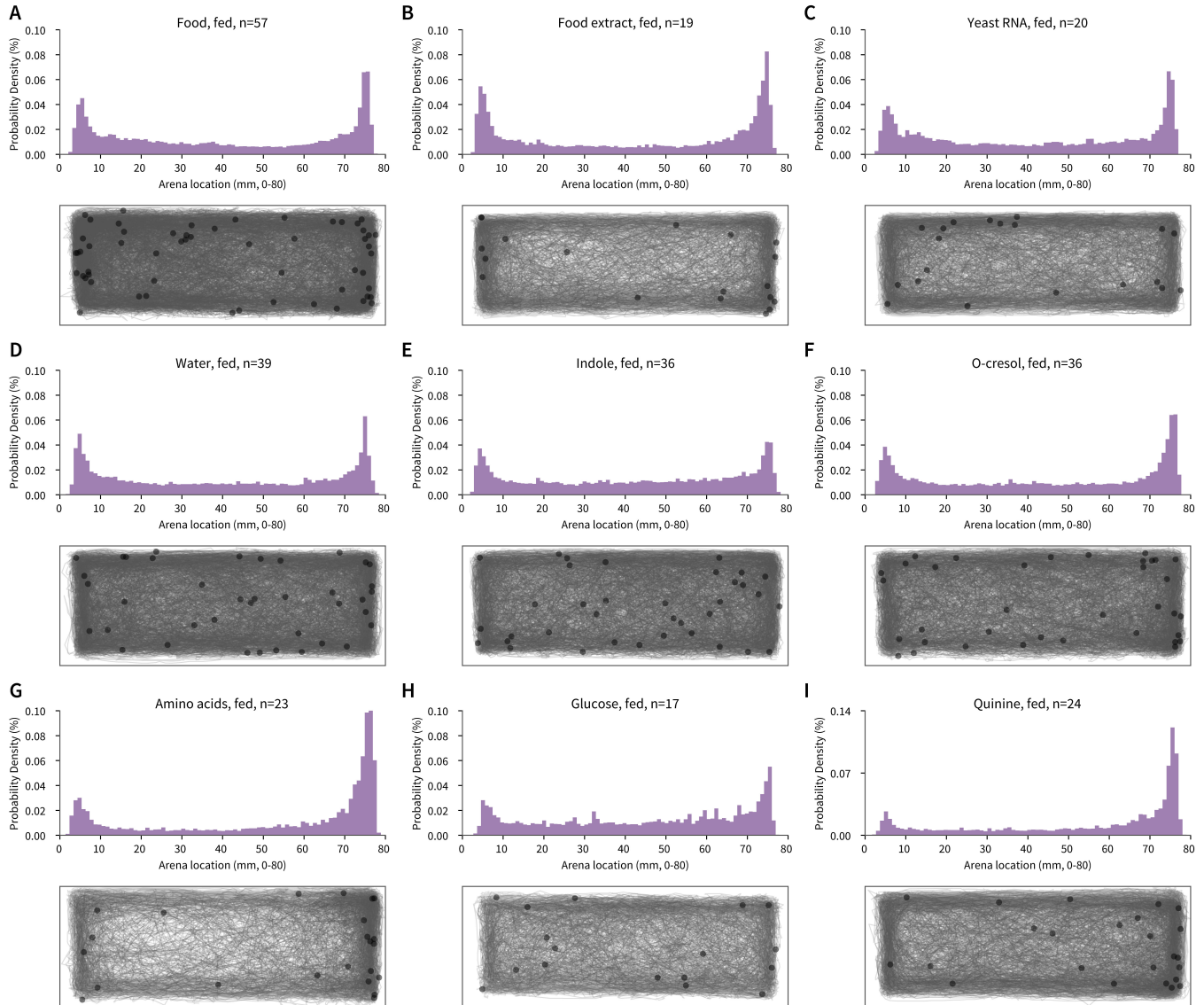


Figure S4: Response of fed larvae to experimental stimuli. A-I: Distribution and trajectories of all starved animals during the experiment phase for food (A), food extract (B), yeast RNA (C), water (D), 100 μ M indole (E), o-cresol (F), amino acid mixture (G), glucose (H), and quinine (I). Although trajectories are shown aggregated into one image for each panel, all animals were tested individually. Scatter points show the position of each animal at the end of the experiment. Note that the high distribution peaks observed at each side of the arena visualize the higher preference for walls observed in fed animals (Fig 4B). As in Fig S3, it is important to note that these histograms show the aggregated position data from all animals throughout the entire 15-minute experiment. Thus, a single animal exhibiting strong attraction or aversion may disproportionately influence this data visualization. For statistical tests reported in this paper, a single preference value was calculated for each animal (Figure 3C) to avoid such effects.

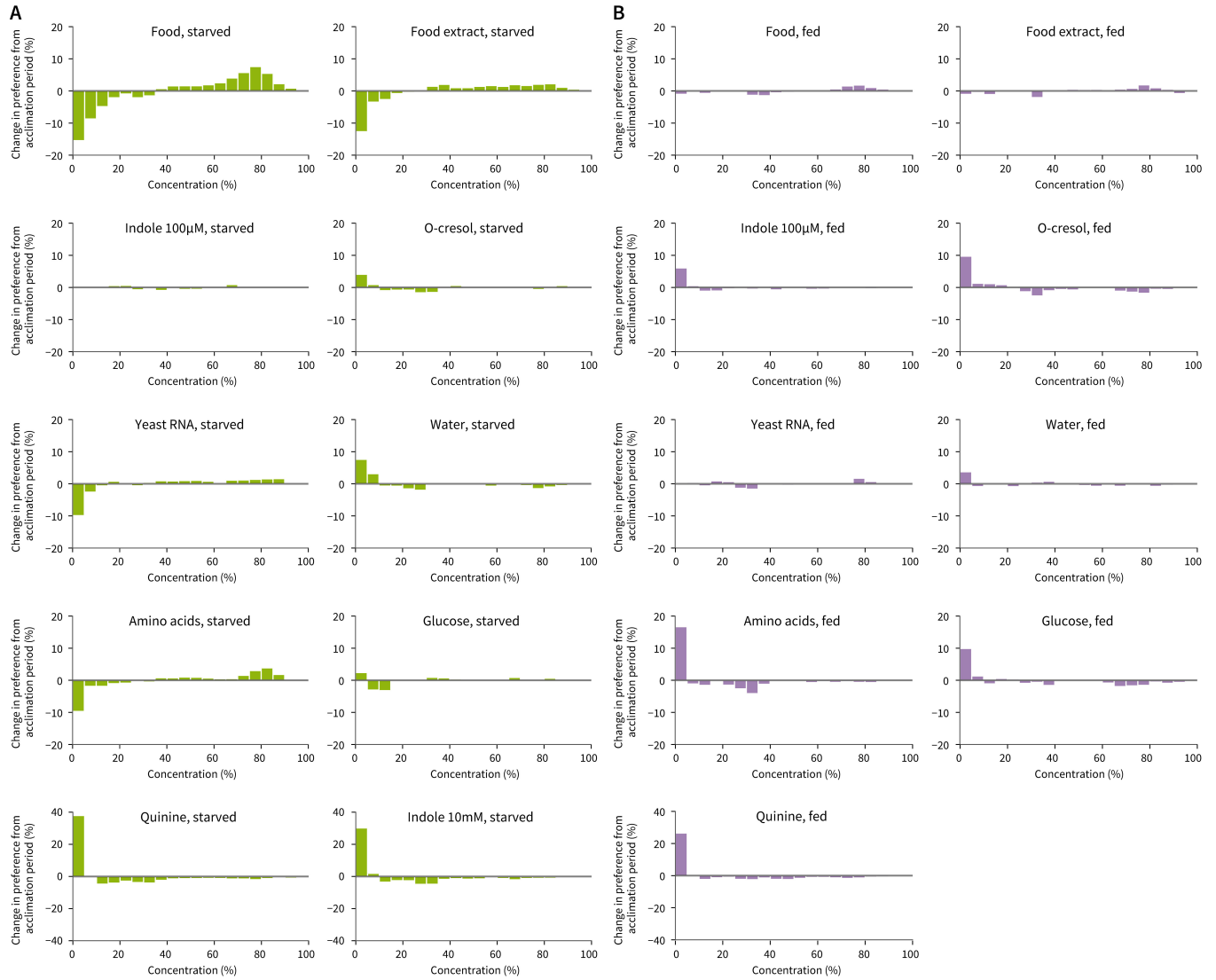


Figure S5: Behaviorally relevant stimuli concentration thresholds for starved and fed larvae. Distribution of starved (**A**) and fed (**B**) animals across the stimulus concentration map. **A, B:** Histograms visualize the change in preference for each concentration bin, normalized to larval distribution during the acclimation phase. This visualization is provided to suggest an estimate for the stimulus concentration thresholds that may be behaviorally relevant for larvae. As in Fig S3 and S4, it is important to note that these histograms show the aggregated position data from all animals throughout the entire 15-minute experiment. Thus, a single animal exhibiting strong attraction or aversion may disproportionately influence this data visualization. For statistical tests reported in this paper, a single preference value was calculated for each animal (Figure 3C) to avoid such effects.

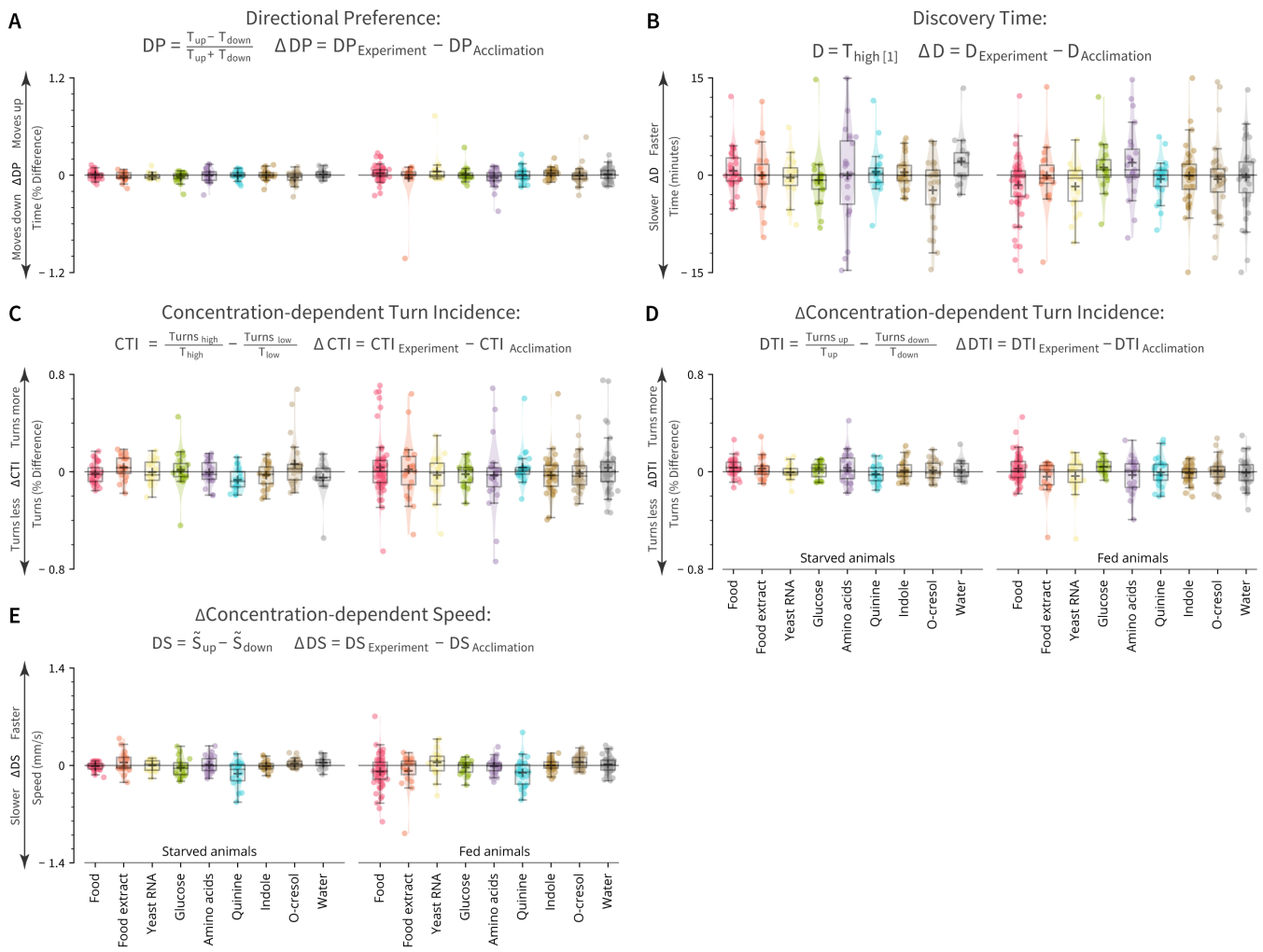


Figure S6: Larval behavior is not consistent with chemotaxis or klinokinesis search strategy models. **A-E:** Box plots for the population median \pm 1 quartile, population mean (+ marker) and mean response for each individual (dots). We observed no significant changes across stimuli for any of these five behavioral metrics ($p > 0.05$, Kruskal-Wallis test). Equations above plots denote how the behavioral metrics were calculated. **A:** Directional Preference ΔDP , difference in time (T) moving up or down the concentration map. **B:** Discovery time ΔD , time (T) elapsed before initial encounter of high concentration ($\geq 50\%$). **C:** Concentration-dependent Turn Incidence ΔCTI , difference in turning rate at high and low local concentrations. **D:** ΔCTI , difference in turning rate while moving up or down concentration. **E:** ΔDS , difference in mean speed (\tilde{S}) while moving up or down the concentration map.

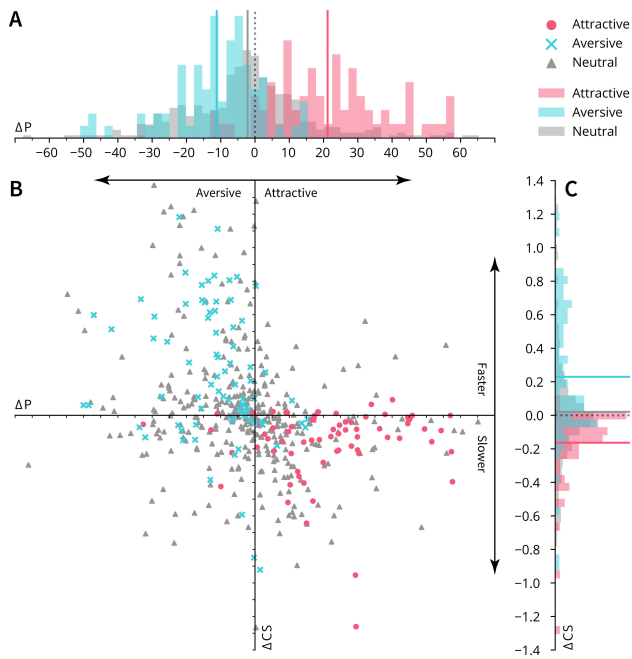


Figure S7: Larval stimulus preference is correlated to concentration-dependent movement speed. **A:** Normalized frequency histograms of ΔP . Mean response to aversive, neutral, and appetitive cues are visualized as solid vertical lines in the corresponding color. A dotted black line at zero indicates the expected outcome if the added stimulus had no effect on larval behavior. **B:** Larval preference (ΔP) significantly correlates with Concentration-dependent Speed (ΔCS). Results from all experiments are shown grouped into three categories: attractive (pink: food, food extract, and yeast RNA in starved larvae), aversive (blue: quinine in fed and starved larvae; o-cresol in fed larvae), and neutral (grey: water, indole, glucose, and amino acids in fed and starved larvae; o-cresol in starved larvae; food, food extract, and yeast RNA in fed larvae). **C:** As in B, except for normalized frequency histograms of larval ΔCS .

	Radius	Frequency	Examples
i	<5cm	27.8% of habitats	Ant traps
ii	5-9cm	9.7% of habitats	Tin cans, bottles
iii	9-17cm	32.3% of habitats	Jars, bowls, vases
iv	17-20cm	3.1% of habitats	Plates, pails

Table S1: Ecologically realistic habitat sizes analyzed through computational modeling. A range of habitat sizes were selected from a literature search of realistic habitat sizes for *Ae. aegypti* larvae ([46] and references therein).

Supplemental Materials and Methods

501 Insects

502 Wild-type *Ae. aegypti* (Costa Rica strain MRA-726,
503 MR4, ATCC Manassas Virginia) were maintained in a
504 laboratory colony as previously described [47]. Experiment
505 larvae were separated within 24 hours of hatching
506 and reared at a density of 75 per tray (26x35x4cm).
507 One day before the experiment, 4-day-old larvae were
508 isolated in FalconTM 50mL conical centrifuge tubes
509 (Thermo Fischer Scientific, Waltham, MA, USA) contain-
510 ing ~15mL milliQ water. Starved larvae were de-
511 nied food for at least 24 hours before the experiment.
512 Animals that died before eclosion or pupated during
513 the experiment were omitted. Because it was not pos-
514 sible to detect younger larvae using our video track-
515 ing paradigm, we mitigated possible age-related be-
516 havioral confounds by standardizing the age of exper-
517 imental larvae.

518 Selection and Preparation of Odorants

519 Odorants (indole, o-cresol) were prepared at 100 μ M in
520 milliQ water (Aldrich #W259306; Aldrich #44-2361)
521 - a concentration previously shown to be significantly
522 attractive to *An. gambiae* mosquito larvae [23]. In-
523 dole was also prepared similarly at 10mM, a concen-
524 tration that is significantly aversive to *An. gambiae*
525 larvae [23]. Quinine hydrochloride was prepared at
526 10mM in milliQ water (Aldrich #Q1125). Larval food
527 (Petco; Hikari Tropic First Bites) was prepared at
528 0.5% by weight in milliQ water and mixed thoroughly
529 before each experiment to resuspend food particles.
530 To prepare the food extract solution, 0.5% food was
531 dissolved in milliQ water for one hour and filtered
532 through a 0.2 μ m filter (VWR International #28145-
533 477). For the yeast RNA solution, total RNA from
534 *Saccharomyces cerevisiae* yeast was prepared at 0.1%
535 by weight in DEPC-treated, autoclaved 0.2 μ m filtered
536 water (Aldrich #10109223001; Ambion #AM9916).
537 Yeast RNA, food, and food extract were prepared fresh
538 daily. Glucose and the amino acid mixture were pre-
539 pared at concentrations previously shown to be op-
540 timal for rearing *Ae. aegypti* larvae [27]: D-(+)-
541 Glucose (Aldrich #G8270) was prepared at 10g/L, and
542 the amino acid solution consisted of L-lysine (Aldrich
543 #L5501, 0.66g/L), L-tryptophan (Aldrich #T0254,
544 0.36g/L), L-histidine (Aldrich #H8000, 0.25g/L), L-
545 leucine (Aldrich #L8000, 1g/L), L-isoleucine (Aldrich
546 #I2752, 1.12g/L), L-threonine (Aldrich #T8625,
547 0.75g/L), L-methionine (Aldrich #M9625, 0.7g/L),
548 L-valine (Aldrich #V0500, 1.2g/L), and L-arginine
549 (Aldrich #A8094, 0.39g/L). Although chemicals dif-
550 fuse at different rates depending on molecular size
551 and physico-chemical properties, diffusion coefficients
552 in water were unavailable for the majority of mixtures
553 chemicals tested. Therefore, it is important to note
554 that our chemical diffusion map is an approximation

555 of the actual chemosensory environment experienced
556 by larvae. Nonetheless, active behavior of the larva
557 modified the chemical distribution in the arena to such
558 a degree that any differences would be negligible.

559 Statistical Analyses

560 Statistical analyses were performed in R version 3.5.1
561 [48]. A Bonferroni-Holm correction was applied to all
562 statistical analyses. A non-parametric Mann-Whitney
563 test was used to compare body length of fed and
564 starved males and females, because a Shapiro-Wilk
565 normality test demonstrated that the data was not
566 normally distributed ($p<0.05$) (Fig S1A). Linear least
567 squares regression was used to assess the effect of
568 time of day to animal speed, time spent moving, and
569 time spent near walls during the acclimation phase
570 (Fig S1B-D). Paired-samples Welch's t-tests were used
571 to compare the median chemical concentration cho-
572 sen by the larvae throughout the 15-minute experi-
573 ment to the behavior of the same larvae through-
574 out the 15-minute acclimation phase. This prefer-
575 ence metric was also quantified as a single value (ΔP ,
576 $P_{Experiment} - P_{Acclimation}$, Fig 3, Fig S4). For all sub-
577 sequent analyses on behavioral mechanisms, larval be-
578 havior during the acclimation phase was subtracted
579 from larval activity during the experiment phase to
580 normalize for differences between individuals and lar-
581 val preference for corners and walls. When inves-
582 tigating potential differences between attraction and
583 aversion behaviors, we grouped stimuli into cues that
584 elicited significant attraction ($\Delta P>0$, $p<0.05$), signif-
585 icant repulsion ($\Delta P<0$, $p<0.05$), or neutral response
586 ($p\geq0.05$). A non-parametric Kruskal-Wallis test was
587 used to compare behavioral metrics among these three
588 stimuli classes, because a Shapiro-Wilk normality test
589 demonstrated that the data was not normally dis-
590 tributed ($p<0.05$) (Fig 3D, Fig S3, Fig S4). These
591 other behavioral metrics included Directional Prefer-
592 ence (ΔDP), defined as the difference in time moving
593 up or down the concentration map; Discovery time
594 (ΔD), defined as the time elapsed before initial en-
595 counter of high ($\geq50\%$) concentration of the stimulus;
596 Concentration-dependent Speed (ΔCS), defined as the
597 difference in speed at high ($\geq50\%$) and low ($<50\%$) lo-
598 cal concentrations; Δ Concentration-dependent Speed
599 (ΔDS), defined as the difference in speed while mov-
600 ing up or down the concentration map; Concentration-
601 dependent Turn Incidence (ΔCTI), defined as the dif-
602 ference in turning rate (turns per second, turns de-
603 fined as instantaneous change in angle of $>30^\circ$) at high
604 and low local concentrations; and Δ Concentration-
605 dependent Turn Incidence (ΔDTI), defined as the dif-
606 ference in turning rate while moving up or down the
607 concentration map. For statistical analyses, larvae
608 that never entered areas of high concentration were as-
609 signed a ΔD of 15 minutes, corresponding to the end

610 of the experiment, and a Δ CS and Δ CTI of 0 (place-
611 holder values chosen to reduce Type I error). We did
612 not conduct statistical analyses on simulated data, and
613 instead report overall trends in the results throughout
614 the manuscript. This approach was chosen because
615 the large number of replicates, which were necessary
616 for reducing the noise introduced by randomizing the
617 larval starting location, would artificially inflate the
618 significance of statistical comparisons.